SCIENTIFIC REPORTS



OPEN

SUBJECT AREAS:

ELECTRICAL AND ELECTRONIC ENGINEERING

LASERS, LEDS AND LIGHT SOURCES

Received
12 March 2014

Accepted
23 May 2014

Published
10 June 2014

Correspondence and requests for materials should be addressed to S.L. (s.lucyszyn@imperial.ac.uk)

* These authors contributed equally to this work.

Secure thermal infrared communications using engineered blackbody radiation

Xiaoxin Liang[1,2]*, Fangjing Hu[1]*, Yuepeng Yan[2] & Stepan Lucyszyn[1]

[1]Centre for Terahertz Science and Engineering, Department of EEE, Imperial College London, Exhibition Road, London SW7 2AZ, UK, [2]Institute of Microelectronics of Chinese Academy of Sciences, 3 Beitucheng West Road, Chaoyang District, Beijing 100029, PR China.

The thermal (emitted) infrared frequency bands, from 20–40 THz and 60–100 THz, are best known for applications in thermography. This underused and unregulated part of the spectral range offers opportunities for the development of secure communications. The *'THz Torch'* concept was recently presented by the authors. This technology fundamentally exploits engineered blackbody radiation, by partitioning thermally-generated spectral noise power into pre-defined frequency channels; the energy in each channel is then independently pulsed modulated and multiplexing schemes are introduced to create a robust form of short-range secure communications in the far/mid infrared. To date, octave bandwidth (25–50 THz) single-channel links have been demonstrated with 380 bps speeds. Multi-channel *'THz Torch'* frequency division multiplexing (FDM) and frequency-hopping spread-spectrum (FHSS) schemes have been proposed, but only a slow 40 bps FDM scheme has been demonstrated experimentally. Here, we report a much faster 1,280 bps FDM implementation. In addition, an experimental proof-of-concept FHSS scheme is demonstrated for the first time, having a 320 bps data rate. With both 4-channel multiplexing schemes, measured bit error rates (BERs) of $< 10^{-6}$ are achieved over a distance of 2.5 cm. Our approach represents a new paradigm in the way niche secure communications can be established over short links.

Wireless ship-to-ship communications, via optical signalling, was implemented by the British Royal Navy in 1867. This represents an early example of pulsed-banded-noise communications, whereby data is transmitted intentionally within the visible spectral range. Today, the commonwealth navies and NATO forces still use signal lamps when secure radio communications need to be silent or electronic *'spoofing'* is likely. Signalling at night is usually conducted in the near-infrared part of the spectrum, using filtered incandescent light bulbs and requiring night vision sights, minimising the risks of being intercepted or jammed.

Ubiquitous hand-held remote controls also use the near-infrared (NIR); here, signal carrier sources employ light-emitting diodes (LEDs) due to their low cost and high spectral efficiency. Unlike lasers, LEDs emit incoherent radiation and this represents an example of modern pulsed-banded-noise communications. While these commercial applications are very susceptible to being intercepted and jammed, secure line-of-sight (LoS) voice & data links (having very low data rates) are also available for security and military applications. Increasing the level of security is normally achieved through be-spoke encryption of data, while the physical layer may employ standardized NIR hardware platforms that conform to international regulations.

Coherent signal carrier sources are generally preferred for implementing advanced communications systems, as these enable higher levels of modulation and with improved signal-to-noise ratio (SNR)[1–4]. However, implementing laser-based infrared systems are prohibitively large and expensive for most applications. Alternatively, banded-noise carrier generators that are modulated by baseband signals have been introduced in both communications[5] and radar[6,7] systems. For example, with noise radio[5], non-return-to-zero (NRZ) binary phase-shift keying (BPSK) for delayed-division multiple access communications was demonstrated at 2.4 GHz. Here, white noise generation spectrally appears as thermal noise to other radio systems – having a higher level of security, through greater immunity to detection, interception and interference (both natural and man-made) – and is very low cost at microwave frequencies. Noise radar[6,7] offers similar advantages to noise radio. Using wide-band noise in the microwave band, from 1 to 2 GHz, one can achieve high resolution and reduced ambiguities in range and Doppler estimations for applications including covert military surveillance and reconnaissance[6].

Having higher physical layer security in mind, the 19th century ideas of optical signalling and the flashlight[8] are reconsidered here for the 21st century. Nowadays, similar systems using low-cost LEDs and on-off keying (OOK) modulation have been widely used for near-infrared[9] and visible[10–11] communications. In contrast, little has been reported on wireless communications in the thermal infrared spectral region, due to high atmospheric attenu-

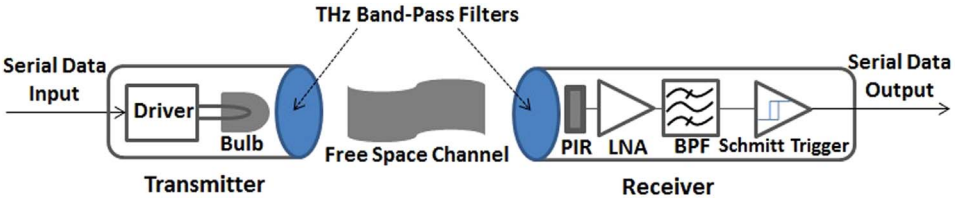


Figure 1 | **Basic architecture for on-off keying '*THz Torch*' wireless link.**

ation beyond a transmission distance of ~1 m in free space. However, such high path losses offer greater immunity to detection, interception and interference; in the same way unlicensed 60 GHz wireless networking (having the 802.11ad IEEE standard[12]) exploits the extremely high atmospheric oxygen (O_2) absorption band.

In the thermal infrared, coherent laser sources are very expensive for most applications; while incoherent LED sources are not widely available due to the lack of appropriate material systems having sufficiently small bandgaps. Moreover, for achieving a minimum level of bit-error rate (BER), increasing the level of transmit power is through higher spectral radiance, within a fixed bandwidth; which may compromise its immunity to detection.

Engineering blackbody radiation (through controlled thermodynamics) can exploit incoherent band-limited noise power within the thermal infrared[13–15]. Here, the transmitter can apply OOK with NRZ pulses to the thermal source across an ultra-wide bandwidth – increasing the level of transmit power can be through higher spectral radiance and/or bandwidth – while pyroelectric infrared (PIR) detectors can operate across this ultra-wide bandwidth. In summary, the thermodynamics-based *'THz Torch'* concept can be used to implement a very low cost short-range wireless link, having an extremely low probability of detection, interception (including code grabbing) and interference (including jamming), making this technology ideal for ubiquitous security applications.

Results

The basic *'THz Torch'* architecture[13] intended for short-range secure wireless communications is shown in Fig. 1. For convenience, this channel transmitter employs five miniature incandescent light bulbs, connected in series, having its thermal noise power (generated from blackbody radiation) channel-filtered. OOK modulation is implemented by either internal (e.g. electrical pulses) or external (e.g. liquid crystal or mechanical) means. At the channel receiver, the incoming band-limited noise power is again filtered by a matching channel filter. A PIR sensor is employed as a square-law detector. The output signal voltage passes through a low-noise amplifier (LNA), baseband band-pass filter (BPF) and then threshold detected using a Schmitt trigger.

With modern communications systems, multiplexing schemes can offer important benefits; including increased overall end-to-end data rates (with band-limited channels) and higher levels of security. For multi-channel operation, a number of standard or bespoke filters can be used to create filter banks for implementing different multiplexing schemes.

In this work, 1 mm thick optical coating filters, sourced from Northumbria Optical Coatings Ltd., are employed to define four non-overlapping frequency bands within the thermal infrared[16]. The measured transmittances for each channel filter are given in Fig. 2, from 20 to 100 THz. The bandwidth, selectivity and transmittance for each channel filter are chosen to create approximately equal levels of band-limited blackbody radiation within each transmission channel.

In order to increase data rates beyond those of individual transmitter-receiver pair channels, frequency division multiplexing (FDM) is one solution. Here, the frequency spectrum is divided up into N non-overlapping frequency bands. The end-to-end serial data stream is converted into N parallel streams, where data is simultaneously sent over the associated free-space channels at the maximum bit rate that the existing enabling technologies can support. After detection, amplification and digitization at the channel receivers, the N output parallel data streams are multiplexed to reconstruct the original transmitted serial data stream; having an overall data rate that is N times that supported by each channel. A simple 4-channel *'THz Torch'* FDM scheme[14] is illustrated in Fig. 3a.

A maximum channel data rate of 320 bps was achieved with the existing non-optimal demonstrator setup; the speed is limited by our be-spoke mechanical chopper, operating at 192 rpm. This corresponds to an effective end-to-end data rate of 1,280 bps. When compared to our previously reported proof-of-concept FDM demonstrator[14], reasons for the x32 improvement in data rate include the use of (1) faster PIR sensors, (2) noise cancelling using dual-PIR sensors and (3) improved low noise post-processing electronics.

To compare channel quality with such multiplexing schemes, BER analysis was performed. Fig. 3b shows the measured overall BER for

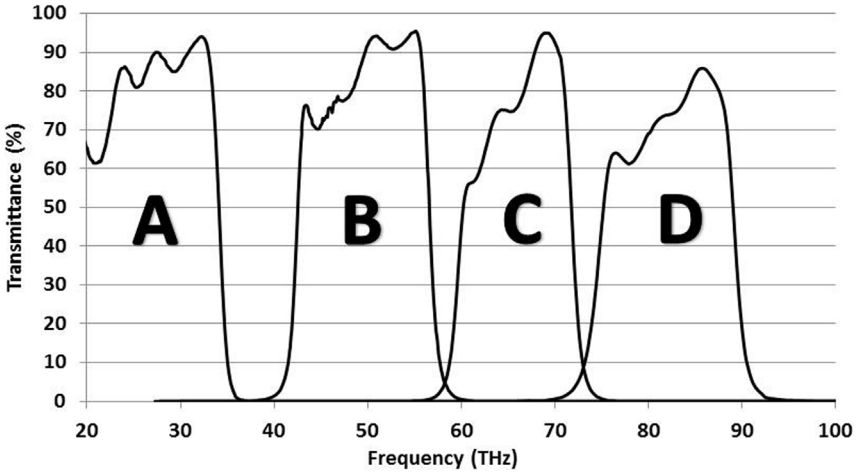


Figure 2 | **Measured transmittance responses for transmission channel (A, B, C and D) filters from Northumbria Optical Coatings Ltd.[16].**

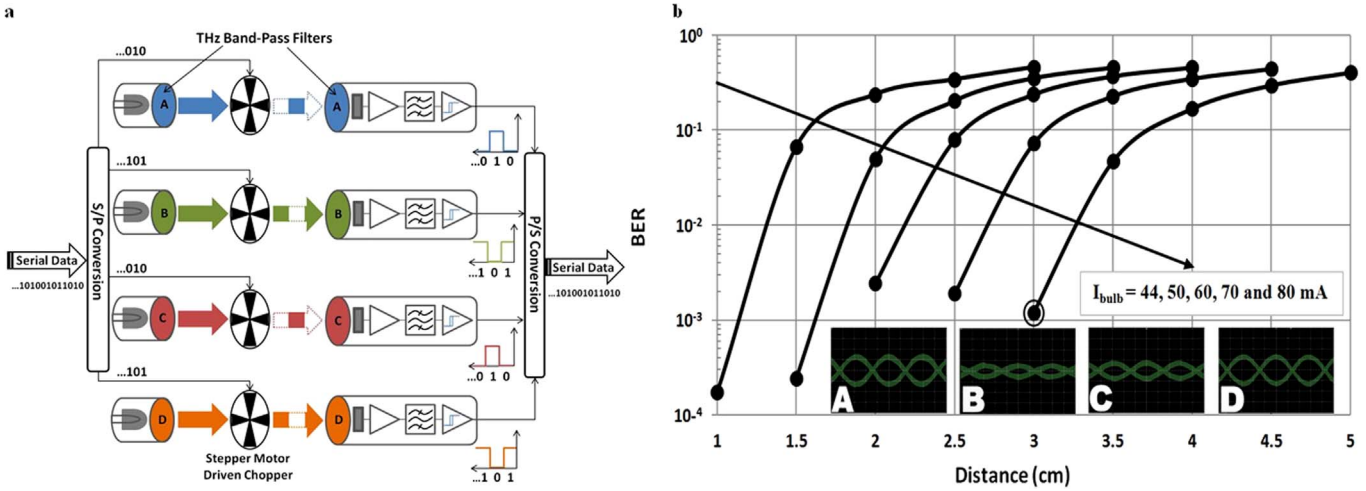


Figure 3 | ***'THz Torch'* FDM scheme.** (a), Basic architecture. (b), Measured overall BER for the 4-channel FDM scheme versus free space transmission distance for different channel transmitter bias currents.

the 4-channel *'THz Torch'* FDM system. For a channel transmitter (i.e. incandescent bulb array) bias current of 44 mA, the BER was measured to be 2×10^{-4} over a distance of 1 cm. As the range increases, the BER becomes progressively worse, due to the spreading loss of the radiated power, as no collimating lenses are employed in this experiment. For an 80 mA bias current, no errors were detected in transmission for distances up to 2.5 cm; and the characteristic BER curve can then be seen at distances beyond 3 cm. The inset of Fig. 3b shows the measured eye diagrams for each of the four channels, labelled in accordance with the channel filter responses given in Fig. 2, having a bias current of 80 mA and a range of 3 cm. It can be seen that the eye is wide open with channels A and D, with the former being slightly noisier due to exposure to more ambient blackbody radiation *seen* within this channel. Channel B has an almost closed eye, which dominates the overall BER performance of the complete system, due to having the lowest band-limited blackbody radiation level. Fortunately, these eye diagrams can be adaptively controlled, by changing the bias currents for each channel, to equalise the output voltage between each channel receiver; thus, optimising the BER performance of the complete multiplexing system.

In addition to FDM, with the same hardware, a frequency-hopping spread-spectrum (FHSS) scheme can be easily implemented to enhance immunity to detection, interception and interference, for secure applications. A simple 4-channel *'THz Torch'* FHSS scheme is illustrated in Fig. 4a. With this proof-of-concept FHSS scheme, the end-to-end serial data stream is transmitted into the same channels as for the FDM system, but only within one channel at any time – dictated by pseudo-random channel allocation. Although there is no advantage in the overall end-to-end data rate for the FHSS scheme, there can be a significant enhancement to security, as will be demonstrated in later experiments.

Slow frequency hopping (SFH) was employed to transmit a 1,000-bit data packet through individual channels, within a single hop. For convenience, a predetermined pseudo-random hopping pattern was applied to both the transmitter and synchronized receiver, to establish the secure end-to-end communications link.

In our FHSS experiment, 2,000 packets were transmitted and the received packets were then analysed. Having a 320 bps channel data rate, the measured overall BER is shown in Fig. 4b. As expected, the overall BER performance is similar to that for the FDM scheme, as the same transmitter and receiver hardware are used in both experiments. In general, however, a slightly better BER performance was observed with FHSS, as only one of four channel links is operating at any time and, therefore, there is no interference due to crosstalk between channels (e.g., direct electromagnetic or mechanical coupling). The results for an experiment to investigate channel crosstalk,

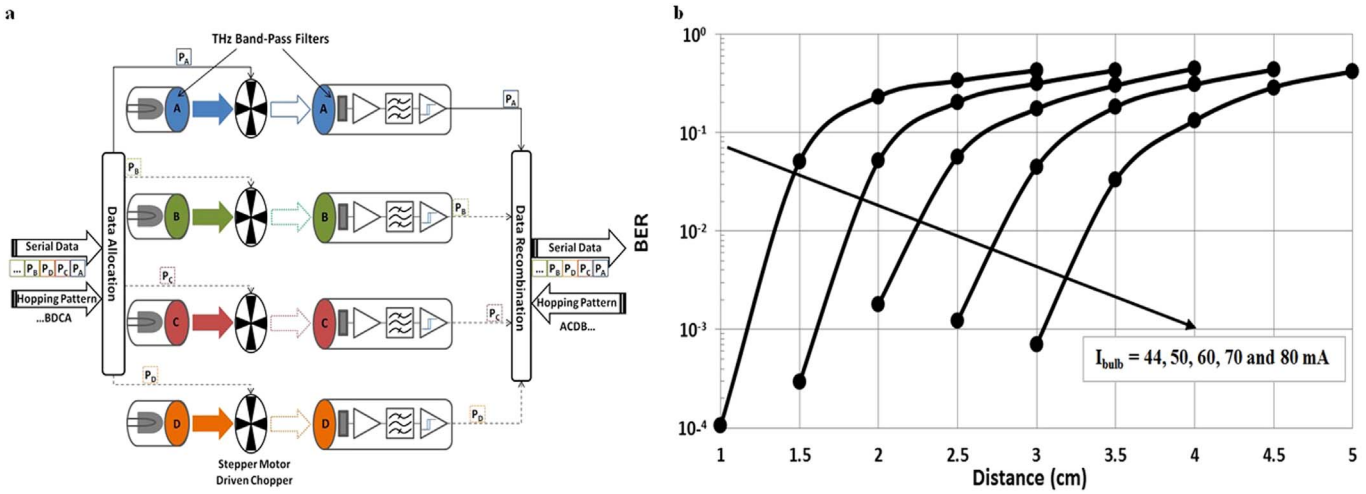


Figure 4 | ***'THz Torch'* FHSS scheme.** (a), Basic architecture. (b), Measured overall BER for the 4-channel *'THz Torch'* FHSS scheme versus free space transmission distance for different channel transmitter bias currents.

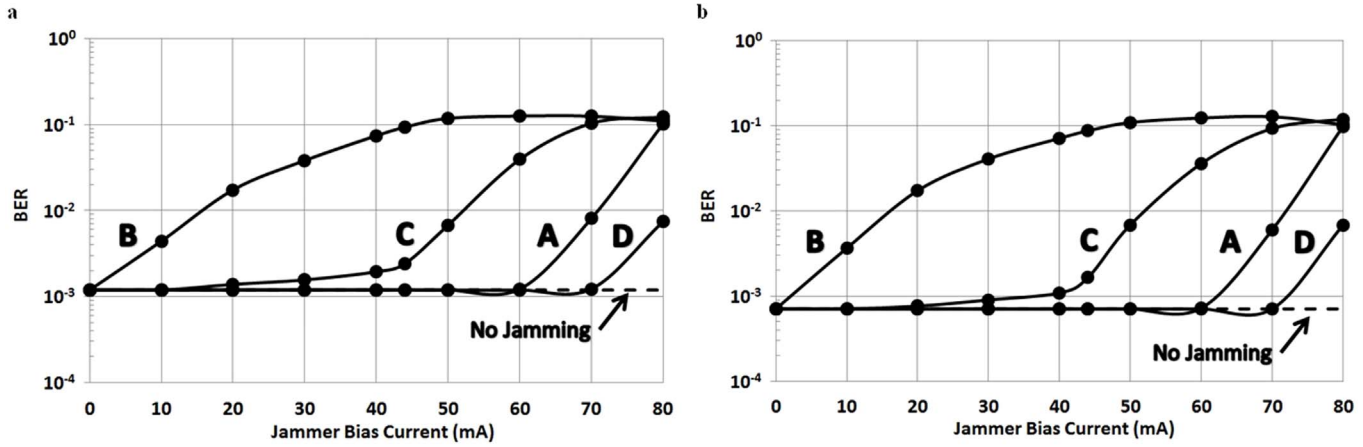


Figure 5 | Experiment for the jamming of different channels for the worst-case condition of the jammer modulation frequency being equal to the channel operating modulation frequency of 320 Hz. (a), Measured overall BER for the 4-channel FDM scheme versus jammer bias current. (b), Measured overall BER for the 4-channel FHSS scheme versus jammer bias current.

due to direct electromagnetic coupling, will be given at the end of this section.

To test the integrity of thermal infrared communications using engineered blackbody radiation, four different experiments were introduced. In the first experiment, a pulse-modulated noise source (i.e. jamming signal) was introduced to each of the four channels separately and the overall BER was recorded for different interfering noise amplitudes (i.e. jammer bias currents). Here, the noise source for the jammer employs the same bulb array as that for the channel transmitter. The effect of the jammer is investigated, one channel at a time, and the resulting overall BER performance is shown in Fig. 5. As expected, the overall BER integrity is similar for both FDM and FHSS schemes. Furthermore, it can be seen that channel D is more robust to the effects of jamming, while channel B is more sensitive. The reason for this is that channel D is the nearest to and channel B is further away from the spectral radiance peak of the primary source of blackbody radiation. As a result, the jamming signal has a greater influence on the weaker signal received from the channel B transmitter. It should be noted that channel A is more robust than channel B, even though its spectral band is furthest away from the spectral radiance peak, because it benefits from a secondary source of blackbody radiation from the glass envelope of the bulbs. One simple solution is to increase the channel transmitter bias currents, by different amounts for the various channels, to effectively balance the overall performance of the complete multiplexing system.

For the second experiment, instead of using the same incandescent light bulb array, the jammer is made from a more expensive miniature thermal noise source (commercially available blackbody infrared radiation emitter INTX 17-0900[17]), which can be pulsed-modulated up to a frequency of 100 Hz (i.e. without the need for the jammer to use a mechanical chopper). With a single INTX 17-0900, having 70% of the maximum input DC power when compared to the previous jamming experiment, the overall output spectral intensity will still be higher than that from the incandescent bulb array. However, as can be seen from the overall BER results shown in Fig. 6, both multiplexing schemes show less sensitive to the jamming signal; the BER increases as the modulation frequency approaches the 320 Hz centre frequency of the baseband BPF. In the existing channel receiver design, a 4th order Sallen-Key Butterworth filter has been implemented. With either a Chebyshev or elliptical filter of the same order or a higher order filter implementation, the integrity of the multiplexing schemes can be further improved; such that the jammer would need to operate much closer to the operating modulation frequency of the channel transmitter to have a significant effect. This sensitivity to modulation frequency can be exploited by a channel receiver that can be reconfigured for more than one modulation frequency, introducing more resilience to mitigate the effects of a jamming signal.

With the third experiment, the possibility of interception by an intruding receiver will be investigated. Here, for convenience, an

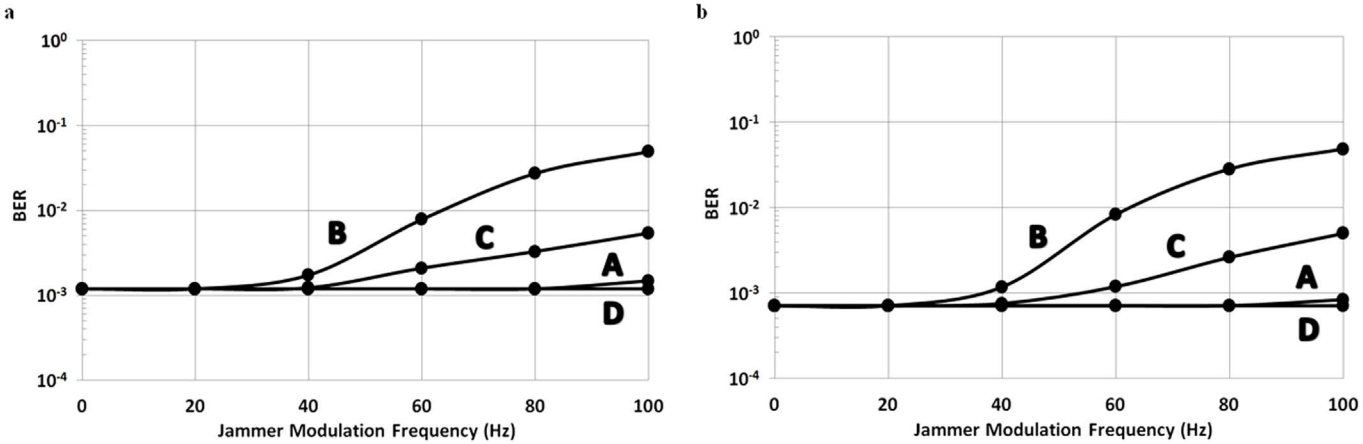


Figure 6 | Experiment for the jamming of different channels with a commercially available blackbody infrared radiation emitter. (a), Measured overall BER for the 4-channel FDM scheme versus jammer modulation frequency. (b), Measured overall BER for the 4-channel FHSS scheme versus jammer modulation frequency.

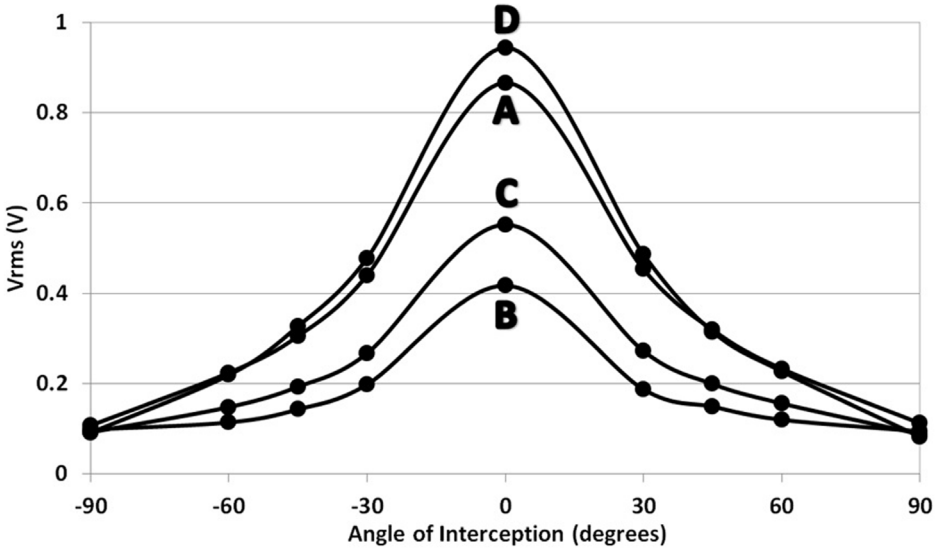


Figure 7 | Experiment for the interception of different channels showing the measured output RMS voltage from the intruding receiver positioned at various angles from normal incidence (the intended channel receiver has been removed from this experiment).

intruding receiver is located in the horizontal plane of the established communications link. The measured output RMS voltage *Vrms* from the intruding receiver positioned at various angles from normal incidence is shown in Fig. 7, for each of the four channels. It can be seen that the output voltages, at normal incidence, correspond in amplitude to the BER performances for each channel. As the off-axis angle increases the output voltage rolls off. With our existing demonstrator setups, having angles of interception within $\pm 45^{\circ}$, it is theoretically possible to intercept the transmitted channel data. However, in practice, since the recommended communications link is confined to a free space transmission distance $R \lesssim 1$ m, the size of both the intended channel and intruding receivers limit how close the interceptor can be positioned to normal incidence. Furthermore, with the use of collimating lenses at the channel transmitters, the beamwidth of the transmitted power would be confined and this would dramatically reduce the likelihood of interception. To get closer to normal incidence, the interceptor would have to be located at a further distance from the intended channel receiver; however, the detected power advantage would be offset because of the $1/R^2$ spreading loss dependency and by the possibility of signal blockage from the intended channel receiver.

With the last experiment, the effects of channel crosstalk are quantified. Each channel receiver is separately aligned, at normal incidence, to the four channel transmitters; this represents the worst-case condition, as there is no spatial displacement introduced between the different channels. The measured output RMS voltage *Vrms* for each channel receiver can be seen in Fig. 8a for different transmit channels. It can be seen that the output voltages, along the main diagonal, correspond in amplitude to the BER performances for each channel. The off-diagonal values represent worst-case channel crosstalk leakage. This can be represented by the calculated channel crosstalk rejection, shown in Fig. 8b. In the existing multiplexing scheme implementations, the high levels of out-of-band rejection seen in Fig. 2 are sufficient to provide high levels of channel crosstalk rejection. However, since channel crosstalk rejection is defined by the ratio of received power from an wanted channel P_{RX_wanted} to that from the unwanted channel $P_{RX_unwanted}$, if P_{RX_wanted} is low for a fixed value of $P_{RX_unwanted}$ then the calculated crosstalk rejection will be artificially low. With this experiment, the worst-case crosstalk rejection of 6.7 dB exists when the channel B receiver detects the weak P_{RX_wanted} and the significant $P_{RX_unwanted}$ from channel A. While the output power from the channel D transmitter is higher than that for channel A, the level of out-of-band rejection is greater at channel D because of its larger spectral separation from channel B. Values for channel crosstalk rejection will increase by increasing the channel transmitter bias current for channel B.

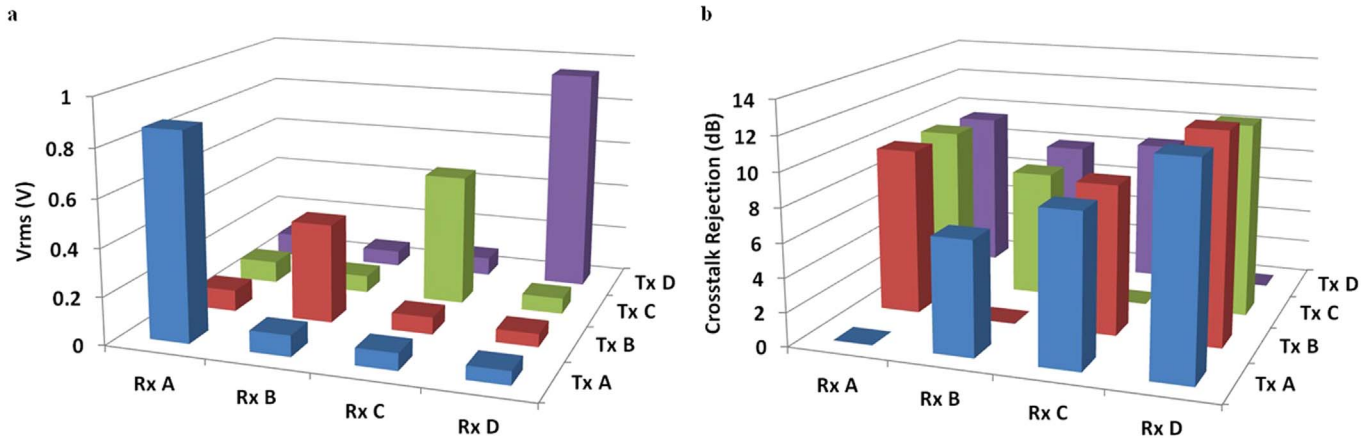


Figure 8 | Experiment for worst-case channel crosstalk. (a), Output RMS voltage for each receive (Rx) channel for different transmit (Tx) channels. (b), Calculated channel crosstalk rejection.

Discussion

In this article, we have demonstrated 4-channel *'THz Torch'* FDM and FHSS schemes for implementing short-range secure wireless communications based on the OOK modulation of band-limited blackbody radiation within the thermal infrared. For the FDM scheme, an end-to-end data rate of 1,280 bps was obtained with an overall BER of 10^{-4} over a 1 cm distance for a 44 mA bias current. This BER performance was improved by applying a higher channel transmitter bias current. For example, with 80 mA, the BER is $<10^{-6}$ for the same distance and this increased to $\sim 10^{-3}$ as the transmission range increases to 3 cm. The first proof-of-concept FHSS demonstrator showed an effective data rate of 320 bps and a slightly improved overall BER. The performance of these system demonstrators can be easily enhanced through the independent control of the channel transmitter bias currents. Moreover, adopting forward error correction (FEC) coding algorithms can further reduce the overall BER for these schemes[18,19].

It has been shown that, in order to undermine the inherent immunity to interference and interception, both the jammer and intruding receiver, respectively, must be designed to meet the same channel spectral bandwidth and operating modulation frequency specifications. With the largely unregulated part of the thermal infrared spectrum, a communications link can be designed to a be-spoke set of specifications that may not be known, *a priori* to the jammer/interceptor; while reconfigurable techniques can be introduced to further enhance the integrity of the *'THz Torch'* system.

With both FDM and FHSS demonstrators, the data rate was ultimately limited by the rotational speed of our mechanical choppers, while the transmission distance is limited by spreading loss and channel transmitter bias currents. With the former, faster external modulators can be employed (e.g., spatial light modulator). With the latter, collimating lenses can be used to increase transmission distances by an order of magnitude. Preliminary results of a single-channel *'THz Torch'* wireless link have demonstrated data rates of $>$1,000 bps over a distance of $>$10 cm using potassium bromide (KBr) convex lenses. In addition, more channels can be employed to overcome limited response times for a single PIR sensor.

By exploring a diverse range of methods, significant enhancements to both data rate and free space transmission distance can be expected. Our approach represents a new paradigm in the sense that 19th century physics can be exploited with 20th century communications schemes for low-cost 21st century ubiquitous security and defence applications in the thermal infrared. More specifically, we have applied known principles to implement transmitter and receiver front-end hardware that is not based on either electronics or optics, but on thermodynamics. Moreover, data transmission has been performed in a part of the electromagnetic spectrum that is not known for wireless communications; within which we have demonstrated complex multiplexing schemes.

Methods

Experimental setup. To perform the OOK modulation of the incoherent band-limited blackbody radiation, for convenience, four customized choppers were employed – each independently driven by their stepper motor (SY35ST36-1004A). A single microcontroller (LPC1768) was used to control all four stepping drivers (DM320C). The end-to-end binary data stream was generated in software (MATLAB®) and then loaded into the microcontroller. Band-limited blackbody radiation was transmitted through a slot in the chopper if the data bit was at logic 1 and blocked by a blade if the data bit was at logic 0. The four transmitter-receiver pairs are spatially aligned to create non-interfering (low channel crosstalk) short-range LoS wireless links. In all instances, the distance between the chopper blades and the transmitter's filter was fixed at 5 mm, while the distance between the chopper blades and the channel receiver was allowed to vary.

BER measurement. In these experiments, an end-to-end binary data stream having 2×10^6 bits was used. With the FDM scheme, 0.5×10^6 bits were sent over each channel. With the FHSS scheme, channel selection was assigned pseudo-randomly, according to a hopping pattern, but on average the same number of bits was sent over each channel. The analogue output from the channel receiver's Schmitt trigger (having voltage levels of almost $\pm$ 5*V*) was input to the microcontroller. The microcontroller has an internal analogue-to-digital converter, to sample and digitally record the quantized levels – for later threshold detection from one centrally-positioned sample point per bit (i.e., values greater than zero representing logic 1 and less than zero representing logic 0). The received data set was then compared with the originally transmitted data set, for subsequent BER analysis. The overall BER performance was evaluated for channel transmitter bias currents from 44 to 80 mA and distances from 1 to 5 cm. In the case where there was no recorded transmission errors for the 2×10^{-6} bit data set, the corresponding BER was considered to be $<10^{-6}$ and, therefore, not shown in Figs. 3b and 4b. With bigger data sets, smaller values of BER can be recorded.

Jamming measurement #1. An additional pulse-modulated noise source is introduced to each channel in turn, to act as an unwanted jammer to one of the channel receivers; however, while having an identical incandescent bulb array source to that of a channel transmitter, the optical filter is removed for it to have a spectral bandwidth that covers all channels. Moreover, since the filter at the jammer is removed, it will have a 5 dB increase in the level of output power for the same bias current within any of the channels; the 40% minimum aperture blockage and 72–84% transmittances from the filter are avoided. However, at the channel receiver, the received signal power from the jammer will be attenuated, due to the off-axis angle of incidence.

(1) The channel transmitter has a fixed location (0° from normal incidence and 3 cm distance to the PIR detector) and a fixed bias current of 80 mA and voltage of 2.484 V (giving a DC power of 199 mW for each bulb, corresponding to a total channel transmitter input DC power of 994 mW). (2) With our large be-spoke mechanical choppers, it is not possible to introduce an extra chopper to change the modulation frequency of the jamming signal. Therefore, the same chopper is used for both the channel transmitter and jammer. As a result, the jammer operates with maximum effectiveness; having the same 320 Hz modulation frequency and 50% duty cycle, while being approximately 180° out-of-phase with the channel transmitter. (3) The jammer is at a fixed location (45° from normal incidence and 3 cm distance to the channel receiver's detector).

Jamming measurement #2. The jammer (INTX 17-0900) is at the same location as with the previous jamming experiment, with the same duty cycle of 50%, and has a bias current of 117 mA and voltage of 5.9 V (corresponding to a total input DC power of 690 mW).

Interception measurement. The channel transmitter has the same fixed location and bias current as with the jamming experiments. With the intruding receiver located in the horizontal plane of the established communications link, the output RMS voltage is recorded at angles of interception from $-90°$ to $+90°$.

Crosstalk measurement. The channel transmitter has the same fixed location and bias current as with the jamming and interception experiments.

1. Greffet, J.-J. *et al.* Coherent emission of light by thermal sources. *Nature* **416**, 61–64 (2002).
2. Federici, J. & Moeller, L. Review of terahertz and subterahertz wireless communications. *J. Appl. Phys.* **107**, 111101 (2010).
3. Elgala, H., Mesleh, R. & Haas, H. Indoor optical wireless communication: potential and state-of-the-art. *IEEE Commun. Mag.* **49**, 56–62 (2011).
4. Koenig, S. *et al.* Wireless sub-THz communication system with high data rate. *Nat. Photon.* **7**, 977–981 (2013).
5. Haartsen, J. C., Meijerink, A., Bekkaoui, A., Taban, A. & Tauritz, J. L. Novel wireless modulation technique based on noise. in *IEEE Symp. on Communications and Vehicular Technology.* (SCVT, 2004) (Date of access: 09/01/2014).
6. Thayaparan, T. & Wernik, C. Noise radar technology basics. in *Defence Research and Development.* (DTIC, 2006) (Date of access: 10/01/2014).
7. Surender, S. C. & Narayanan, R. M. UWB noise-OFDM netted radar: Physical layer design and analysis. *IEEE Trans. Aerosp. Electron. Syst.* **47**, 1380–1400 (2011).
8. Misell, D. inventor; The American Elec, assignee. Electric Device. United States patent *US Patent* 617,592, 1898 Mar 12.
9. Kahn, J. M. & Barry, J. R. Wireless infrared communications. *Proc. IEEE* **85**, 265–298 (1997).
10. Komine, T. & Nakagawa, M. Fundamental analysis for visible-light communication system using LED lights. *IEEE Trans. Consum. Electron.* **50**, 100–107 (2004).
11. Hoa, L.-M. *et al.* 100-Mb/s NRZ Visible Light Communications Using a Postequalized White LED. *IEEE Photon. Technol. Lett.* **21**, 1063–1065 (2009).
12. IEEE 802.11ad, Wireless LAN Medium Access Control (MAC) and Physical (PHY) Layer Specification: Enhancements for Very High Throughput in the 60 GHz Band (2012) (Date of access: 23/01/2014).
13. Lucyszyn, S., Lu, H. & Hu, F. Ultra-low cost THz short-range wireless link. *in MTT-S Int. Micro. Workshop Series on Millimeter Wave Integration Tech.* 49–52 (IEEE, 2011).
14. Hu, F. & Lucyszyn, S. Ultra-low cost ubiquitous THz security systems. in *Proc. of the Asia-Pacific Micro. Conf.* 60–62 (IEEE, 2011).
15. Hu, F. & Lucyszyn, S. Improved 'THz torch' technology for short-range wireless data transfer. in Proc. *Int. Wireless Symp.* 1–4 (IEEE, 2013).

16. Northumbria Optical Coatings Ltd., Online catalogue. http://www.noc-ltd.com/catalogue (2011) (Date of access: 12/10/2011).
17. Electro Optical Components, Inc., Online catalogue. http://www.eoc-inc.com/infrared_source.htm (2014) (Date of access: 20/05/2014).
18. Vucic, J., Kottke, C., Habel, K. & Langer, K.-D. 803 Mbit/s visible light WDM link based on DMT modulation of a single RGB LED luminary. in *Opt. Fiber Comm. Conf.* (OSA, 2011).
19. Azhar, A. H., Tran, T.-A. & O'Brien, D. A. Gigabit/s Indoor Wireless Transmission Using MIMO-OFDM Visible Light Communications. *IEEE Photon. Tech. Lett.* **25**, 171–174 (2013).

Acknowledgments

This work was partially supported by the China Scholarship Council (CSC). Authors also thank Feng Wang, at the Institute of Microelectronics of Chinese Academy of Sciences (China), and Joshua Elsdon at Imperial College London (UK) for their advice.

Author contributions

X.L. implemented the hardware, software coding and BER analysis and wrote this manuscript. F.H. developed the *'THz Torch'* concept and its multiplexing schemes, implemented the hardware, performed the experiments and wrote this manuscript. Y.Y. provided logistical support for coding and BER analysis. S.L. conceived the *'THz Torch'* concept and its multiplexing schemes, designed the methodologies for all the experiments, directed the research and wrote this manuscript.

Additional information

Competing financial interests: The authors declare no competing financial interests.

How to cite this article: Liang, X.X., Hu, F.J., Yan, Y.P. & Lucyszyn, S. Secure thermal infrared communications using engineered blackbody radiation. *Sci. Rep.* **4**, 5245; DOI:10.1038/srep05245 (2014).

This work is licensed under a Creative Commons Attribution-NonCommercial-NoDerivs 3.0 Unported License. The images in this article are included in the article's Creative Commons license, unless indicated otherwise in the image credit; if the image is not included under the Creative Commons license, users will need to obtain permission from the license holder in order to reproduce the image. To view a copy of this license, visit http://creativecommons.org/licenses/by-nc-nd/3.0/